Biomimetic supramolecular fibers exhibit water-induced supercontraction **

*Yuchao Wu,[‡a] Darshil U. Shah,[‡b] Baoyuan Wang,[a] Ji Liu,[a], Xiaohe Ren[a], Michael H. Ramage[b] and Oren A. Scherman[a] **

Abstract: *Spider silk is a fascinating material, combining high strength and elasticity that outperforms most synthetic fibers. Another intriguing feature of spider silk is its ability to 'supercontract', shrinking up to 50% when exposed to water. This is likely on account of the entropy-driven recoiling of secondary structured proteins when water penetrates the spider silk. In contrast, humidity driven contraction in synthetic fibers is difficult to achieve. Here, inspired by the spider silk model, we report a supercontractile fiber (SCF) which contracts up to 50% of its original length at high humidity, comparable to spider silk. The fiber exhibits up to 300% uptake of water by volume, confirmed via environmental scanning electron microscopy (ESEM). Interestingly, the SCF exhibits tunable mechanical properties by varying humidity, which is reflected by the prolonged failure strain and the reversible damping capacity. This smart supramolecular fiber material provides a new opportunity of fabricating biomimetic muscle for diverse applications.*

Natural systems frequently exploit intricate multiscale and multiphasic structures to generate properties which exceed those generally achievable by man-made systems.[1,2] For example, spider dragline silk tends to outperform other natural fibers and most man-made filaments.[3,4] More interestingly, spider silk is able to 'supercontract' at high humidity, with contraction $>$ 50% of its original length.[5–7] Supercontraction is thought to be induced by the entropy-driven revoiling of molecular chains.[8–12] In analogy, most man-made fibers undergo thermal induced shrinkage leading to changes in mechanical properties.[13,14] Humidity driven contraction in synthetic fibers is rarely seen on account of a 'frozen' molecular network in the fiber. Recently, we reported drawing a supramolecular fiber from a self-assembled multi-phase hydrogel at high water content (98%).[15] The fiber exhibits a good combination of tensile properties as well as damping capacity. More importantly, its underlying structure can be readily manipulated to produce novel fiber materials with a range of properties.

We report a supercontractile fiber (**SCF**) that is capable of contracting up to 50% of its original length at high humidity, comparable to spider silk. In comparison to the previously reported supramolecular fiber where the polymer chains were held together solely through dynamic, physical interactions, the **SCF** is imparted with a second network of covalent crosslinks (Figure 1). The resulting **SCF** is not only resilient to water, but also shows stimuli-responsiveness with humidity. The fiber exhibits up to 300% uptake of water by volume at high humidity, confirmed by environmental scanning electron microscopy (ESEM). Moreover, the **SCF** undergoes a cyclic relaxation-contraction response to wetting and drying, similar to spider silk. This type of fiber material provides a new opportunity of fabricating biomimetic muscle for diverse application, ranging from humanoid robots and prosthetic limbs to exoskeletons.

The fabrication of **SCF** was accomplished in two steps. Fibers were initially drawn from a hydrogel composite, followed by a UV treatment at room temperature. The hydrogel is primarily formed by host-guest interactions with cucurbit[8]uril (CB[8]), consisting of methyl viologen (MV) functionalized polymer (P1, 1*wt*%) grafted onto silica nanoparticles, napthol (Np) functionalized hydroxyethyl cellulose (P2, 1*wt*%), CB[8] (0.5*wt*%) and photoinitiator (0.1*wt*%, see ESI Figures S1-3 for synthetic procedures). The constituents serve different purposes: the CB[8] is a supramolecular macrocycle, crosslinking P1 and P2 in aqueous media by forming a dynamic heteroternary complex with the pendant guest molecules on both polymers. This induces the desired viscoleatstic behavior required for directly drawing fibers with high aspect ratio from the hydrogel.[15] In addition, P2 is functionalized with methacrylic anhydride (MA) for further UV crosslinking in the fiber matrix. The resulting fiber is imparted with a double network, including the physical interactions between P1 and P2 and covalent crosslinks within P2.

The efficacy of UV crosslinking was studied in both hydrogel and fiber states. The mechanical properties of the

** This work was supported by the Engineering Physical Sciences Research Council (EPSRC) EP/K503496/1 and EPSRC Programme Grant(NOtCH, EP/L027151/1) and a Translational Grant EP/H046593/1 as well as a Leverhulme Trust Programme Grant (Natural Materials Innovation); Mr Y. Wu was funded EPSRC EP/L504920/1.

* [‡] These authors contributed equally to this work.
[a] Y. Wu, Dr. J. Liu, B. Wang, X. Ren and Prof. O. A. Scherman
Melville Laboratory for Polymer Synthesis
Department of Chemistry, University of Cambridge
Lensfield Road, Cambridge, CB2 1EW, UK
Fax: +44 (0)1223 334866; E-mail: oas23@cam.ac.uk
[b] D. U. Shah and M. H. Ramage
Department of Architecture, University of Cambridge
1 Scroope Terrace, Cambridge CB2 1PX

Supporting information for this article is available on the WWW under or from the author.

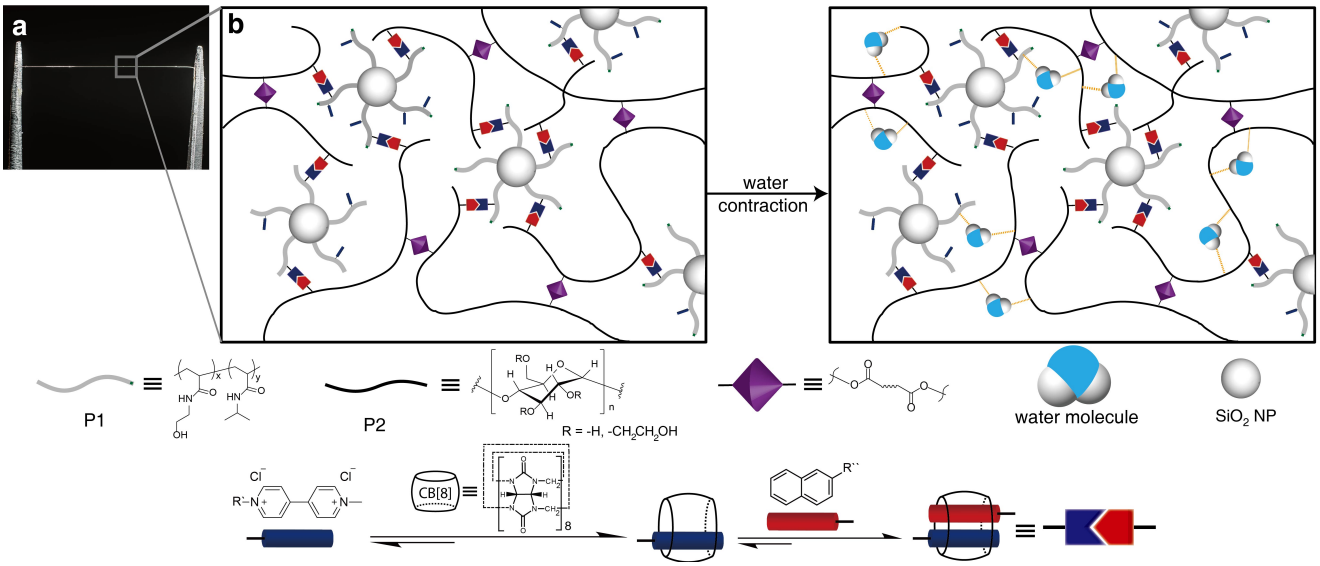

Figure 1 a, Photograph of the supercontractile fiber (**SCF**). **b**, schematic illustration of **SCF** undergoing supercontraction at high humidity. Water molecules penetrate into the fiber matrix and interact with the hydrophilic moieties. The covalent crosslinks ensure the stability of wet fiber, while the dynamic crosslinks enable the movement of polymer chains. Thus, water induces the polymer chains to reconfigure toward higher entropy and cause the entire fiber to contract.

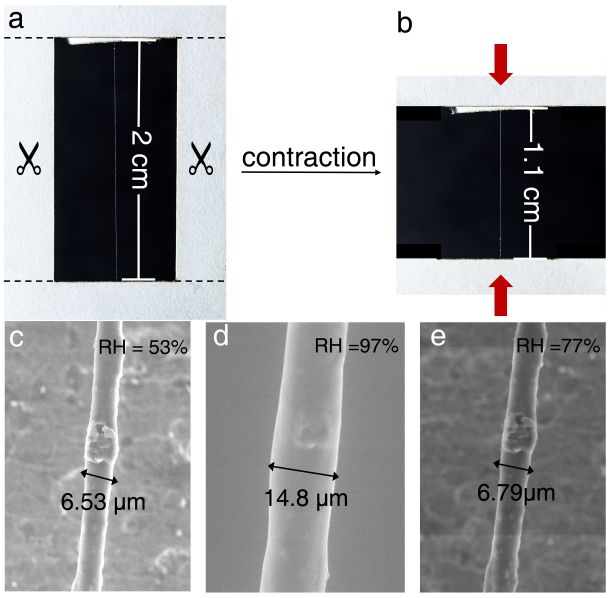

Figure 2 a-b, Photographs of **SCF** undergoing supercontraction at high humidity, RH $>$ 70%. **c-e**, Environmental SEM images of the **SCF** at different humidity, difference in diameter indicating different amount of water uptake inside the **SCF**.

hydrogels were characterized through rheological measurements. Strain dependent oscillatory rheology of the hydrogel before UV treatment displays a broad linear viscoelastic region (storage moduli G′ $>$G″, Tan $\delta \approx 0.75$, ESI Figure S4a). After UV treatment, the value of G′ increases dramatically to more than twice its original state (Tan $\delta \approx 0.66$), indicating additional crosslinks inside the hydrogel composite (ESI Figure S4c). This is correlated with a decrease in the elasticity of the hydrogel as it cannot yield high aspect ratio fibers. Similarly in the frequency dependent oscillatory rheology, a large increase in G′ across the whole range of frequencies was observed in the hydrogel before and after the UV treatment (ESI Figure S4b and d). In terms of the fiber state, the success of UV crosslink was clearly demonstrated by the stability test of the fiber in water. Fibers that were produced from the hydrogel without further crosslinking could be easily solubilized upon rehydration on account of the fiber network being held together solely by dynamic interactions. In comparison, the fiber after UV treatment remained stable without any collapse in the fiber matrix (ESI Figure S7). This further confirmed that the **SCF** was reinforced by the additional covalent crosslinks.

Interestingly, the **SCF** was observed to contract at high humidity, similar to spider silk. As shown in Figure 2a and b, upon introducing high humidity, the **SCF** contracts from an original length of 2 cm to 1.1 cm. The contraction could achieve values up to 50% (average 42 $\pm$ 7%), and it is independent of fiber diameter (ESI Figure S8). ESEM was used to further investigate the **SCF** with respect to humidity variation in an effort to explain its unique contraction behavior. As polymeric materials are usually assumed to be incompressible, we expect no volumetric change, and therefore changes in length (supercontraction) must be twinned with changes in diameter (swelling). Figure 2c depicts a section of the fiber (D = 6.53 μm) at a relative humidity of 53%. As the humidity increased (RH = 97%), the diameter expanded significantly to 14.82 μm. By calculating the net volume of the fiber, we could estimate the volume of water uptake (1.4 nL/cm). This represents a large amount of water that rapidly penetrated into the fiber matrix without breaking the network. Furthermore, as the relative humidity dropped,

the diameter of the swollen fiber decreased accordingly, indicating an entirely reversible process of water uptake and release (see video S1). This is possibly on account of the co-existence of dynamic network inside the fiber, including polymer chains entanglement, slipping and host-guest interactions of CB[8]. In addition, the **SCF** did not contract when immersed into a non-polar solvent such as toluene, even though organic solvent also causes the **SCF** to swell (ESI Figure S9). Therefore, contraction of the **SCF** could be attributed to its uptake of water at high humidity. When water molecules penetrate into the fiber matrix, they disrupt the hydrogen bonding within the polymer chains. This disruption does not cause any collapse or breakage in the **SCF** on account of the crosslinked polymer network. Yet it is sufficient to allow the polymer chains to reconfigure gaining in entropy and causing the entire fiber to suddenly contract in length while expanding in overall volume. The **SCF** now behaves like a filled rubber with a relatively low modulus, which is confirmed by the following mechanical tests. A similar model has also been proposed in spider silks.[5]

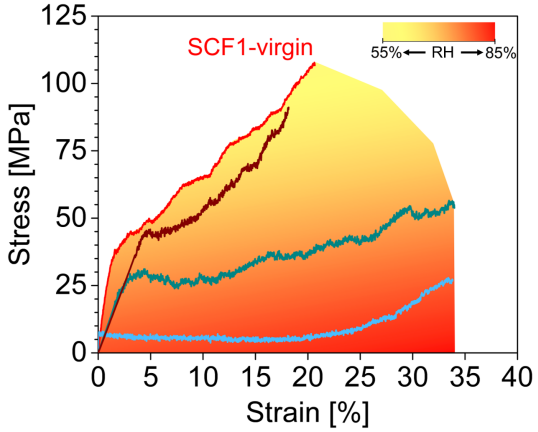

Figure 3 Tensile engineering stress-strain response of supercontractile fibers produced with 1 hr UV crosslinking duration (SCF1) tested a various humidity levels. SCF1-virgin identifies the stress-strain curve for an as-produced fiber at 55% RH.' SCF1 tested at various humidity levels. See ESI Figure S12 for comparison between initial modulus, strength and failure strain.

The UV crosslinking of the fibers prevents them from dissolving in water and also substantially alters their dynamic mechanical behavior. Tensile tests reveal that the **SCF** have significantly lower modulus and strength in comparison to the uncross-linked fibers, with the failure strain remaining unchanged (ESI Figure S11). An increasing in crosslink density, resulting from varying UV crosslinking duration leads to similar observations (ESI Figure S11). The drop in modulus and strength with crosslinking is presumably a result of multiple factors. First, crosslinks may have a defect trapping effect.[16–18] Defects, such as internal voids,[15] may be locked during the formation of the covalent crosslink network and act as microcracks during tensile loading, leading to premature failure. Second, crosslinking may cause initial decrease in crystallinity of the system and introduce flexible moieties. This has been identified as a cause reduction in the modulus of crosslinked polyvinyl alcohol,[19] a semi-crystalline polymer that can be used as an alternative to the semi-crystalline HEC used here to produce supramolecular fibers.[15] Third, it is envisaged that the formation of a second chemical network through covalent crosslinks may alter the molecular stretching behavior within the fiber, for example by restricting some of the dynamic mechanisms associated with the purely non-covalent interactions of the uncrosslinked fiber. Nevertheless, the degree of crosslinking can be viewed as a tool to tune the mechanical behavior of the fibers, as is evidenced by the range of stress-strain profiles that can be generated (ESI Figure S11).

Most interesting were our observations on the effects of humidity on fiber properties. We have already shown that, like spider silks, our crosslinked supramolecular fibers exhibit substantial supercontraction in water. Moisture substantially alters fiber mechanical properties: while 'dry' fibers tested at RH = 55% (SCF1-virgin fibers) have stiffness, strength and failure strain of 2.1 $\pm$ 0.6 GPa, 110 $\pm$ 27 MPa and 19.8 $\pm$ 4.7%, respectively, 'wet' fibers (at RH = 75-80%) exhibited very low stiffness of 0.17 $\pm$ 0.07 GPa, low strength of 30 $\pm$ 11 MPa, and high failure strains of 31.1 $\pm$ 9.4% (Figure 3, Supplementary Figure 12). Furthermore, in comparison to the classic linear elastic region at low (<2%) strains observed for the 'dry' fibers, the 'wet' fibers present an extended region (up to 25% applied strain) in which the fiber deforms substantially for minute increases in applied stress. The 'J-shaped' stress-curve curve of the latter is similar to elastomers, and biomaterials such as human skin and muscle tissue. Indeed, a family of stress-strain profiles are observed with varying levels of relative humidity (Figure 3, ESI Figure S12). Moreover, by re-drying fibers from RH = 80% to RH = 60%, we found that the effects of humidity were reversible, with the fiber stress-strain profiles returning to their virgin dry state (at RH = 55%).

Intriguingly, the humidity response of our supramolecular fiber mimics the behavior of major ampullate spider silks.[8,20] Major silks generate an envelope of stress-strain plots when spun under different conditions, namely humidity level and spinning rate. A number of studies have computationally simulated this behavior by using structure-defining parameters such as the degree of supercontraction, also referred to as the coefficient of shrinkage, and the order/disorder fraction, also known as the alignment parameter.[8,20] It has been proposed that water, and other polar solvents like ethanol, 'plasticize' the silk, leading to an increase in the internal free volume and thereby increasing mobility and dispersion of and damage to inter- and/or intramolecular hydrogen bonds. Eventually, plasticization increases the disordered fraction (and decreases the ordered fraction) of the biopolymer, which consequently affects supercontraction.[8,20–23] We envisage that as in spider silks, water disrupts non-covalent interactions, particularly hydrogen bonding, in our supramolecular fibers.

The cyclic response and damping behavior of the

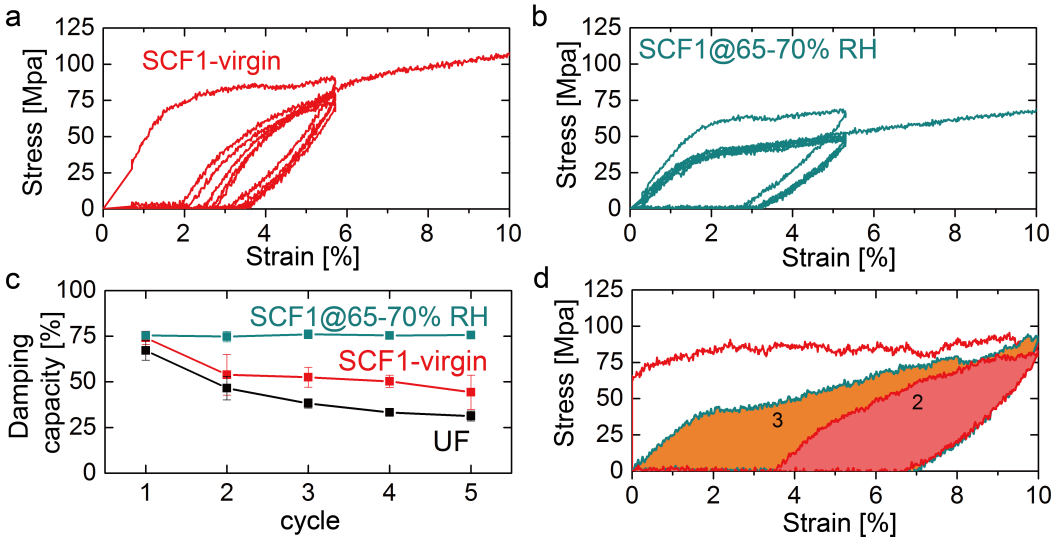

Figure 4 a, Cyclic response of an SCF1-virgin fiber (at RH = 55%) exhibits hysteresis loops decreasing in area with every cycle, alongside an increasing recovery strain and permanent set ('permanent' deformation). **b**, However, if after each unloading cycle, RH is increased to 65-70%, and the fiber is re-loaded thereafter, the fiber exhibits a 'reset' and stable response, with a constant high damping capacity at 75%, and no permanent set. **c**, The evolution of damping capacity (ratio of damping energy to stored energy) with loading cycles is depicted for three different fibers: uncrosslinked fibers (UF; from[15]), SCF1-virgin (at RH = 55%), and SCF1 rehydrated to 65-70% RH before every reload cycle. **d**, The 'reset' can be implemented at any cycle. In this case, we were able to reset the properties at every alternate cycle (3,5, and so on).

supramolecular fibers were evaluated through multiple load-unload-reload tests (Figure 4). When tested at RH = 55%, the crosslinked fiber exhibited a damping capacity of 74.1 ± 3.6%, measured by the ratio of the damping energy to the stored energy in each load-unload cycle (Figure 4a and 4b). This was even higher than the impressive initial damping capacity of the uncrosslinked fiber of 67.2 ± 5.3%, both of which exceed spider silks and viscose (Figure 4c).[15] However, we observe that similar to spider silks, substantially lower damping capacities were registered for subsequent cycles, 44.3 ± 9.4% by the fifth cycle for the crosslinked fiber, and 31.2 ± 2.8% for the uncrosslinked fiber (Figure 4c).[15] This is likely due to molecular rearrangement upon loading and unloading,[15] and the manifestation of a permanent set from plastic deformation. Excitingly, we observed that water-induced supercontraction enables elimination of any permanent set from the loading history. In essence, exposing the fiber to a high moisture environment (RH > 75%) 'reset' the fiber properties, presumably by resetting the molecular organization. Upon subsequent equilibration of the fiber at RH = 65-70% (during a 5 minute dwell period in the unload-reload cycle), we were able to obtain a consistent damping capacity of 75.4 ± 4.9% for every load-unload cycle Figure 4c). Comparing the load-unload-reload stress-strain plots for the crosslinked fiber without (Figure 4a) and with (Figure 4b) the high-moisture environment resetting step clearly shows the removal of any permanent set, and a stable hysteresis response with a larger, constant hysteresis loop, for the latter. This further reflects the improved and stabilized damping performance. Figure 4d shows the ability to exercise control over the damping behavior by, resetting the properties every alternate cycle. It is well-known among silk experts that proteinacious spider silk dragline fibers also exhibit such tunability and control in static and dynamic properties through interactions with water.[8,21–23] While the evolutionary function and advantage of this is not known for spider silks,[23,24] applications of such smart functional materials can be envisioned in sensors and biomedical applications.

SCF exhibits an average pre-stress of 20.0 ± 8.4 MPa (ESI Figure S13). To demonstrate an analogy of our **SCF** fibers with muscle fibers, multiple SCFs were aligned and joined as a fiber bundle to conduct weight lifting experiments (Figure 5a-b). As shown in Figure 5c, the hanging weight is 5 mg, after spraying water on the fiber bundle, it contracted and lifted the weight 0.5 cm (12.5%) within a second. This represents an approximate 10 MPa in stress. In addition, the weight lifting can be repeated for multiple cycles (Figure 5d), after resetting the length of the fiber bundle.

Water is a key resource and tool in nature. Spider silks, for instance, are produced from a dope where water is the solvent, and water is also used by the spider to control properties for a range of functions. Learning how to effectively use water to produce such low-energy, high-performance fibers will be key in future sustainable fiber processing. Development of supramolecular fibers formed from hydrogels (with 98 *wt%* water) with emergent properties including supercontraction are important and pioneering scientific step changes in material science.

In conclusion, we demonstrated the supercontractile fiber by introducing a double network, consisting of a dy-

namic network governed by polymer chain entanglement and CB[8] host-guest interactions as well as a covalent network that enhances resilience against water penetration. The underlying dynamic interactions allow the reconfiguration of polymer chains within the fiber matrix. The penetrated water molecules induce contraction of the **SCF** up to 50%, which is comparable to spider silk. Moreover, similar to spider silk, the mechanical properties of **SCF** is tunable according to the humidity level. The **SCF** is a good example for developing emerging fiber materials, such as sensors and artificial muscles. We envision the alteration of chemistry and processing technology offer limitless opportunities towards biomimetic materials.

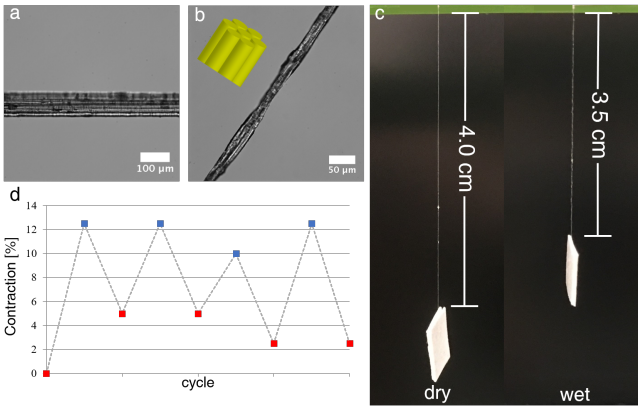

Figure 5 a-c, Micrograph of the **SCF** bundle, imitating a muscle fiber to lift weight (5 mg). **d**, Recyclability diagram of the fiber bundle showing weight lifting can be repeated in multiple cycles.

References

[1] P. Egan, R. Sinko, P. R. Leduc, S. Keten, *Nat. Commun.* **2015**, *6*, 7418.

[2] J. C. Nawroth, H. Lee, A. W. Feinberg, C. M. Ripplinger, M. L. Mccain, A. Grosberg, J. O. Dabiri, K. K. Parker, *Nat. Biotechnol.* **2012**, *30*, 792–797.

[3] M. Heim, D. Keerl, T. Scheibel, *Angew. Chem.* **2009**, 3584–3596.

[4] R. Ene, P. Papadopoulos, F. Kremer, *Soft Mater.* **2009**, *212*, 4568–4574.

[5] T. A. Blackledge, C. Boutry, S.-c. Wong, A. Baji, A. Dhinojwala, V. Sahni, I. Agnarsson, *J. Exp. Biol.* **2009**, *2*, 1981–1989.

[6] I. Agnarsson, A. Dhinojwala, V. Sahni, T. A. Blackledge, *J. Exp. Biol.* **2009**, 1990–1994.

[7] C. Boutry, T. A. Blackledge, *J. Exp. Biol.* **2010**, 3505–3514.

[8] Y. I. Liu, Z. Shao, F. Vollrath, *Nat. Mater.* **2005**, *4*, 901–905.

[9] Z. Qin, M. J. Buehler, *Nat. Mater.* **2013**, *12*, 185–187.

[10] Y. Zheng, H. Bai, Z. Huang, X. Tian, F.-q. Nie, Y. Zhao, J. Zhai, L. Jiang, *Nature* **2010**, *463*, 640–643.

[11] X. Huang, G. Liu, X. Wang, *Adv. Mater.* **2012**, 1482–1486.

[12] I. Agnarsson, C. Boutry, S.-c. Wong, A. Baji, A. Dhinojwala, A. T. Sensenig, T. A. Blackledge, *Zoology* **2009**, *112*, 325–331.

[13] C. S. Haines, M. D. Lima, N. Li, G. M. Spinks, J. Foroughi, J. D. W. Madden, S. H. Kim, S. Fang, M. J. D. Andrade, F. Göktepe, Ö. Göktepe, S. M. Mirvakili, S. Naficy, X. Lepró, J. Oh, M. E. Kozlov, S. J. Kim, X. Xu, B. J. Swedlove, G. G. Wallace, R. H. Baughman, *Science* **2014**, *343*.

[14] C. S. Haines, N. Li, G. M. Spinks, A. E. Aliev, J. Di, R. H. Baughman, *Proc. Natl. Acad. Sci. U.S.A.* **2016**, *113*, 11709–11716.

[15] Y. Wu, D. U. Shah, C. Liu, Z. Yu, J. Liu, X. Ren, M. J. Rowland, C. Abell, *Proc. Natl. Acad. Sci. U.S.A.* **2017**, *114*, 8163–8168.

[16] X. Liu, Y. Won, P. X. Ma, *Biomaterials* **2006**, *27*, 3980–3987.

[17] S. Dong, B. Zheng, F. Wang, F. Huang, *Acc. Chem. Res.* **2014**, *47*, 1982–1994.

[18] X. Yan, F. Wang, B. Zheng, F. Huang, *Chem. Soc. Rev.* **2012**, *41*, 6042–6065.

[19] R. Benavente, C. Mijangos, J. M. Peren, M. Krumova, D. Lo, *Polymer* **2000**, *41*, 9265–9272.

[20] F. Vollrath, D. Porter, *Soft Matter* **2006**, 377–385.

[21] J. Perez-Rigueiro, M. Elices, G. Guinea, *Polymer* **2003**, *44*, 3733–3736.

[22] M. Elices, G. R. Plaza, *J. Exp. Biol.* **2005**, *208*, 25–30.

[23] Z. Shao, F. Vollrath, *Polymer* **1999**, *40*, 1799–1806.

[24] M. Elices, G. R. Plaza, J. Pérez-rigueiro, *J. Mech. Behav. Biomed.* **2011**, *4*, 658–669.